30th International Conference
ENGINEERING MECHANICS 2024
Milovy, Czech Republic, May 14 – 16, 2024

AUGMENTED M5 GEOMETRY OF HUMAN VOCAL FOLD IN PHONATORY POSITION – PILOT RESULTS

Hájek P.[*], **Horáček J.**[**], **Švec J. G.**[***]

Abstract: *The presented contribution deals with a newly designed parametric planar geometry of the vocal fold – the augmented M5 model – which is fitted to a real-shaped human vocal fold. The real shape of the vocal fold during a phonatory position for* 112 Hz *was obtained from a plaster cast and was digitized by optical scanning. The geometry model of the vocal fold surfaces was constructed based on the data from the optical scanner and the augmented M5 model was fitted to a coronal slice of the selected vocal fold surface. The equations of the augmented M5 model are explained and its parameters, tuned to the real vocal fold geometry, are provided. The fitting is done in Python 3.8.5 using the* `scipy.optimize.curve_fit` *package, which contains non-linear least squares method. It is shown that the augmented M5 model fits the real data with coefficient* R^2 *close to* 1 *and the tuned parameters are in a good agreement with the overall vocal fold dimensions and with the parameters of the original 2D M5 model.*

Keywords: Vocal fold, M5 geometry, non-linear least squares, curve fitting, phonatory position.

1. Introduction

Computational modeling of human phonation is a demanding task requiring knowledge of the underlying physics, interactions between the vocal folds and fluid flow, materials of the soft tissues and warmer humid air and the geometry of the human larynx. The latter is often simplified to an idealized parametric geometry. Such a parametric geometry of the human vocal fold can be implemented in a code, there is a possibility to tune its parameters, but it can also be physically inaccurate.

There have been numerous attempts, *e.g.* in Titze (1989); Alipour and Scherer (2000); Scherer et al. (2001); Alipour-Haghighi and Scherer (2015); Li et al. (2012); Xue et al. (2014); Wu and Zhang (2016, 2019); Chen et al. (2020), to define the geometry of the human vocal fold using highly simplified geometries as well as relatively complex ones – each was suitable for different approaches in computational or experimental modeling. One of the most widely used geometries is the three-parametric M5 shape of the vocal fold (Scherer et al., 2001). The key part of the planar geometry consists of two circular arcs with a tangent line between them. Although this shape fits the real vocal fold well, the other two tangents representing upper and lower boundary of the vocal fold are too simplified to fit the real shape of the vocal fold. To overcome this limitation, an augmented 2D M5 vocal fold shape is constructed and presented here.

2. Methods

The augmented M5 geometry is based on a plaster cast of the human larynx in the phonatory position at the vocal folds self-oscillation frequency of 112 Hz, which was obtained and described in our previous

[*] Ing. Petr Hájek, PhD.: Institute of Solid Mechanics, Mechatronics and Biomechanics, Brno University of Technology, Technická 2896/2; 616 69, Brno; CZ; Voice Research Laboratory, Department of Experimental Physics, Palacký University Olomouc; 17. listopadu 1192/12; 779 00, Olomouc; CZ, hajek.p@fme.vutbr.cz

[**] Ing. Jaromír Horáček, DSc.: Institute of Thermomechanics of the Czech Academy of Sciences; Dolejškova 1402/5; 182 00, Prague; CZ, jaromirh@it.cas.cz

[***] Prof. RNDr. Jan G. Švec, PhD. et PhD.: Voice Research Laboratory, Department of Experimental Physics, Palacký University Olomouc; 17. listopadu 1192/12; 779 00, Olomouc; CZ, jan.svec@upol.cz

doi: 10.21495/em2024-106

study (Šidlof et al., 2008). The plaster cast (see Fig. 1a) was digitized with an accuracy of 0.1 mm using the SHINING 3D EinScan-SE optical scanner, see Fig. 1b). The resulting stereolithography (STL) geometry model was cut, cleaned and smoothed in GOM Inspect to extract the vocal folds (Fig. 1c) and to obtain the final STL surfaces of the left and right vocal folds in 3D (Fig. 1d).

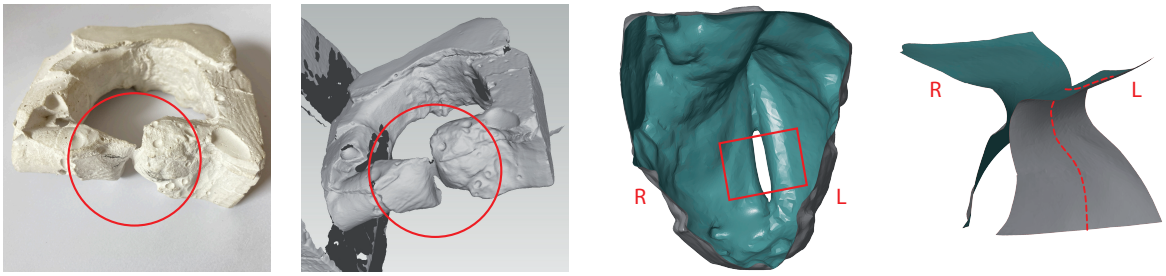

a) *b)* *c)* *d)*

Fig. 1: Stages of digitalization of the plaster cast: a) plaster cast of the human vocal folds (encircled); b) raw digitized geometry of the plaster cast; c) view from the cranio-caudal direction of the extracted vocal folds (cut part is marked) and d) cleaned and smoothed surfaces of the vocal folds (representative slice is marked on the left vocal fold). Left and right vocal folds are labeled.

The left vocal fold from the Fig. 1d) was then processed in Python 3.8.5 using the `numpy-stl` package. The loaded surface of the vocal fold was sliced by the frontal plane to obtain a representative slice of the vocal fold surface. The surface was finally fitted by the augmented M5 geometry model. The fitting was performed using the non-linear least squares method from the `scipy.optimize.curve_fit` package.

2.1. Augmented M5 geometry as a fitting function

Unlike the original three-parametric M5 model (Scherer et al., 2001), the augmented M5 model has eight parameters: R_o, T, Ψ (these are the original M5 parameters, see Fig. 2a) that fully control the geometry between points B–E and R_{AB}, α_{AB}, R_{EF}, β_{EF} and β (these are the added parameters) that control the lower and upper boundary of the vocal fold, which are designed as two circular arcs, see Fig. 2b). Like the original M5 model, also the augmented M5 geometry forms a smooth curve with tangency between each line or arc.

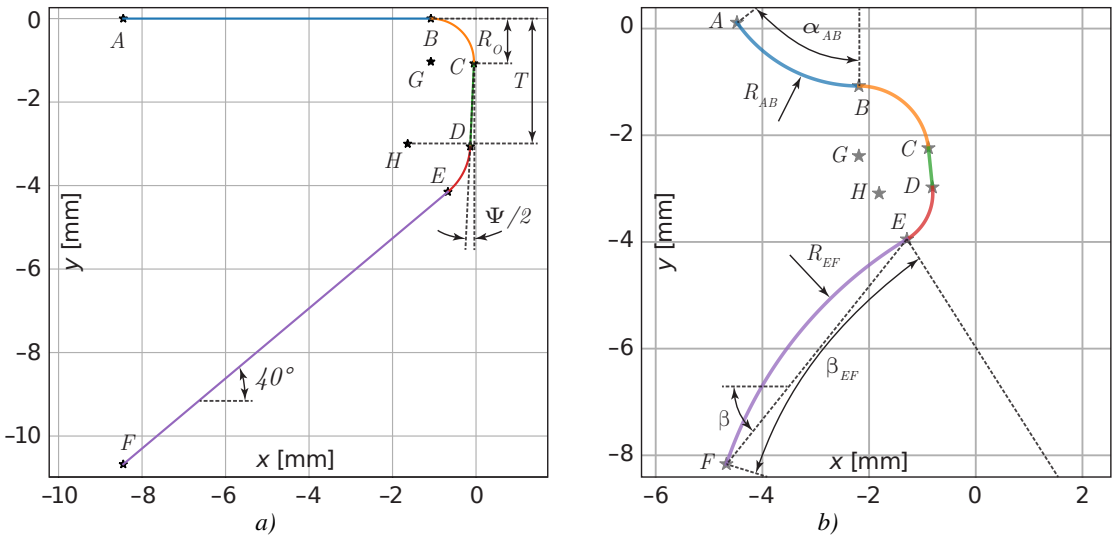

a) *b)*

Fig. 2: Development of the augmented M5 model: a) the original M5 geometry with: $R_o = 0.987\,\text{mm}$, $T = 3.000\,\text{mm}$ and $\Psi = 5\,°$ and b) the augmented M5 geometry with the remaining parameters: R_{AB}, α_{AB}, R_{EF}, β_{EF} and β.

The fitting function is a piecewise-defined function with arcs and a straight line between points A–F. Points G and H are the centers of the two arcs from the original M5 model, see Fig. 2b). The centers of the arcs between points A and B and between E and F are not shown in Fig. 2b), but are labeled by points I and J,

respectively. Since the geometry is planar, each point has two coordinates in x and y denoted by a subscript. The equations of the point coordinates are as follows:

$$A_x = -\left(\frac{W_G}{2} + \frac{R_o}{1-\sin\Psi/2}\right) - R_{AB}\cdot\sin\alpha_{AB}, \tag{1}$$

$$A_y = Y_{off} + R_{AB}\cdot(1-\cos\alpha_{AB}), \tag{2}$$

$$B_x = -\left(\frac{W_G}{2} + \frac{R_o}{1-\sin\Psi/2}\right), \tag{3}$$

$$B_y = Y_{off}, \tag{4}$$

$$C_x = -\left(\frac{W_G}{2} + \frac{R_o}{1-\sin\Psi/2}\right)\cdot(1-\cos\Psi/2), \tag{5}$$

$$C_y = Y_{off} - \frac{R_o}{1-\sin\Psi/2}\cdot(1+\sin\Psi/2), \tag{6}$$

$$D_x = -\left\{\frac{W_G}{2} + \left[T\cdot\left(1+\frac{\sin\Psi/2}{2}\right) - \frac{R_o}{1-\sin\Psi/2}\right]\cdot\tan\Psi/2\right\}, \tag{7}$$

$$D_y = Y_{off} - T\cdot\left(1+\frac{\sin\Psi/2}{2}\right), \tag{8}$$

$$E_x = D_x - T\cdot\left(\frac{\cos\Psi/2}{2} - \frac{\sin\beta}{2}\right), \tag{9}$$

$$E_y = Y_{off} - T\cdot\left(1+\frac{\cos\beta}{2}\right), \tag{10}$$

$$F_x = E_x + R_{EF}\cdot[\sin\beta - \cos(\pi/2-\beta-\beta_{EF})], \tag{11}$$

$$F_y = E_y - R_{EF}\cdot[\cos\beta - \sin(\pi/2-\beta-\beta_{EF})], \tag{12}$$

$$G_x = B_x, \tag{13}$$

$$G_y = Y_{off} - \frac{R_o}{1-\sin\Psi/2}, \tag{14}$$

$$H_x = D_x - T\cdot\frac{\cos\Psi/2}{2}, \tag{15}$$

$$H_y = Y_{off} - T, \tag{16}$$

$$I_x = B_x, \tag{17}$$

$$I_y = Y_{off} + R_{AB}, \tag{18}$$

$$J_x = E_x + R_{EF}\cdot\sin\beta, \tag{19}$$

$$J_y = E_y - R_{EF}\cdot\cos\beta. \tag{20}$$

These equations are derived for programming purposes rather than being in the most elegant form. Besides the eight parameters that control the geometry, there are two parameters W_G (width of the *glottis*) and Y_{off} (y offset) that control an offset of the entire geometry in x and y directions, respectively, and which are necessary for a correct fit with respect to a chosen reference point. The complete geometry is placed in the third quadrant of a plane. The line and the arcs between the points from Eqs. (1) to (20) can be constructed very easily using linear equation and Pythagorean theorems, respectively.

3. Results and Discussion

The fit from a representative slice in the center of the selected vocal fold is shown in Fig. 3 together with the resulting parameters. The augmented M5 geometry (the multicolored line in Fig. 3) fits the real shape (the blue dots in Fig. 3) with coefficient $R^2 = 0.999$. *Glottis* is in a divergent shape with $\Psi < 0$. The angle β is sharper than the angle of $40\,^\circ$ in the original M5 geometry (recall Fig. 2a). The parameters R_{AB} and R_{EF} describe the curvatures of the lower and upper boundaries of the vocal fold and are of the order of mm. The parameters α_{AB} and β_{EF} define the length of the arc of the upper and lower boundary and are at the upper limit of the bounds given in the non-linear least squares method. The parameters R_o, T and Ψ are close to the original parameters stated in Scherer et al. (2001).

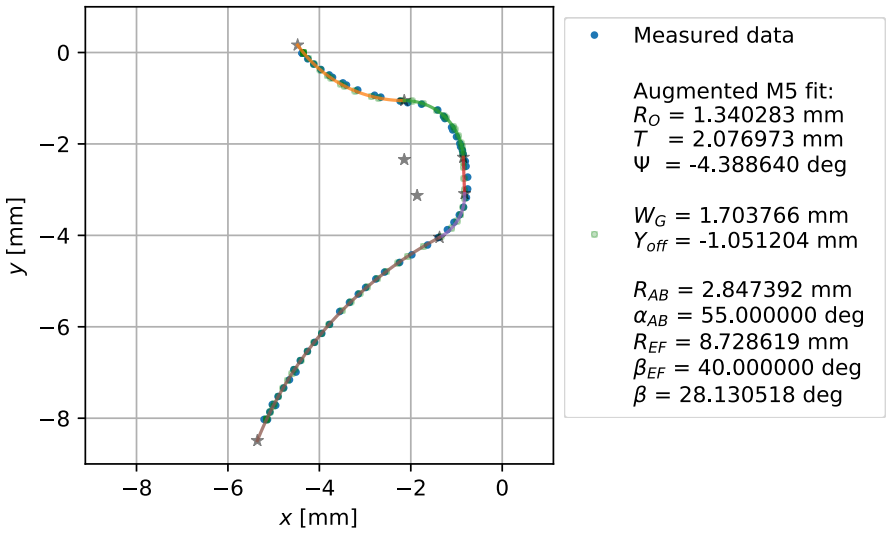

Fig. 3: The augmented M5 geometry fitted on data from the real vocal fold (left) with the resulting parameters (right).

4. Conclusions

The augmented M5 geometry of the vocal fold presented here fits the real shape of the human vocal fold very well, with R^2 better than 0.99. This geometry can be reconstructed from Eqs. (1) to (20) and the resulting parameters given in Fig. 3 and can be used for subsequent numerical or experimental analyses of the human voice production. The fitting code is available on `https://github.com/hajekpc/Augmented-M5-geometry.git`.

Acknowledgment

The study was supported by a grant from the Czech Science Foundation: No. 24-11121S “Redistribution of acoustic energy output in human voice and its effect on vocal folds loading using computer and physical modeling”.

References

Alipour, F. and Scherer, R. C. (2000) Vocal fold bulging effects on phonation using a biophysical computer model. *Journal of Voice*, 14, 4, pp. 470–483.

Alipour-Haghighi, F. and Scherer, R. C. (2015) Time-Dependent Pressure and Flow Behavior of a Self-oscillating Laryngeal Model with Ventricular Folds. *Journal of Voice*, 29, 6, pp. 649–659.

Chen, Y., Li, Z., Chang, S., Rousseau, B., and Luo, H. (2020) A reduced-order flow model for vocal fold vibration: From idealized to subject-specific models. *Journal of Fluids and Structures*, 94, pp. 102940.

Li, S., Scherer, R. C., Wan, M., and Wang, S. (2012) The effect of entrance radii on intraglottal pressure distributions in the divergent glottis. *The Journal of the Acoustical Society of America*, 131, pp. 1371–1377.

Scherer, R. C., Shinwari, D., De Witt, K. J., Zhang, C., Kucinschi, B. R., and Afjeh, A. A. (2001) Intraglottal pressure profiles for a symmetric and oblique glottis with a divergence angle of 10 degrees. *The Journal of the Acoustical Society of America*, 109, 4, pp. 1616–1630.

Šidlof, P., Švec, J. G., Horáček, J., Veselý, J., Klepáček, I., and Havlík, R. (2008) Geometry of human vocal folds and glottal channel for mathematical and biomechanical modeling of voice production. *Journal of Biomechanics*, 41, 5, pp. 985–995.

Titze, I. R. (1989) A Four-Parameter Model of the Glottis and Vocal Fold Contact Area. *Speech Communication*, 8, pp. 191–201.

Wu, L. and Zhang, Z. (2016) A parametric vocal fold model based on magnetic resonance imaging. *The Journal of the Acoustical Society of America*, 140, 2.

Wu, L. and Zhang, Z. (2019) Voice production in a MRI-based subject-specific vocal fold model with parametrically controlled medial surface shape. *The Journal of the Acoustical Society of America*, 146, 6, pp. 4190–4198.

Xue, Q., Zheng, X., Mittal, R., and Bielamowicz, S. (2014) Subject-specific computational modeling of human phonation. *The Journal of the Acoustical Society of America*, 135, 3, pp. 1445–1456.